Multiphase modelling of the growth kinetics of precipitates in Al-Cu alloys during artificial aging

Tohid Naseri , Daniel Larouche , Pierre Heugue , Rémi Martinez , Francis Breton & Denis Massinon

Published online: 19 Aug 2020.

Submit your article to this journal

Article views: 250

View related articles

View Crossmark data

Taylor & Francis
Taylor & Francis Group

Multiphase modelling of the growth kinetics of precipitates in Al-Cu alloys during artificial aging

Tohid Naseri[a], Daniel Larouche[a], Pierre Heugue[a], Rémi Martinez[b], Francis Breton[c] and Denis Massinon[d]

[a]Department of Mining, Metallurgy and Materials Engineering, Aluminum Research Center – REGAL, Laval University, Québec, Canada; [b]Linamar Corporation – The Center, Guelph, Canada; [c]Rio Tinto, Arvida Research and Development Centre, Saguenay, Canada; [d]Linamar Montupet Light Metal Division, Laigneville, France

ABSTRACT

In the aluminum industry, the needs of predictability of the kinetics of precipitation during the artificial aging processes increase as the targeted applications require the maximisation of properties at the lowest costs possible. In this regard, kinetics modelling can be helpful to design the heat treatment processes. Despite using many fitting parameters, available models show a lack of fitting with experimental data, especially for the apparent heat capacity measured at high temperatures by a differential scanning calorimeter (DSC). To address this issue, a mixed-mode model was recently developed for isothermal heat treatment, whereas non-isothermal heat treatment must be considered to compare the calculated results with those measured by isochronal heating in a DSC. In this contribution, the model is extended to non-isothermal heat treatments. To this end, the growth kinetics pathway and sequence of precipitation in a binary Al-Cu alloy have been simulated, optimising the pre-exponential factor and the activation energy of the interfacial mobility of the secondary phases. This calibration of the interfacial mobilities allowed a very good reproduction of the evolution of the apparent heat capacity with temperature. The model and calibrated interfacial mobilities were then used to compute the size evolution of θ' precipitates in an Al-4 wt%Cu. The isothermal growth rates calculated at 4 temperatures were in good agreement with those measured and reported by independent researchers. The good predictability of the model indicates that the assumptions made were suitable and well funded, especially regarding the growth rates of embryos emerging from the subcritical growth regime.

CONTACT Daniel Larouche ✉ Daniel.Larouche@gmn.ulaval.ca 🖳 Department of Mining, Metallurgy and Materials Engineering, Aluminum Research Center – REGAL, Laval University, 1065, ave de la Médecine, Québec, G1V 0A6, Canada

This article has been republished with minor changes. These changes do not impact the academic content of the article.
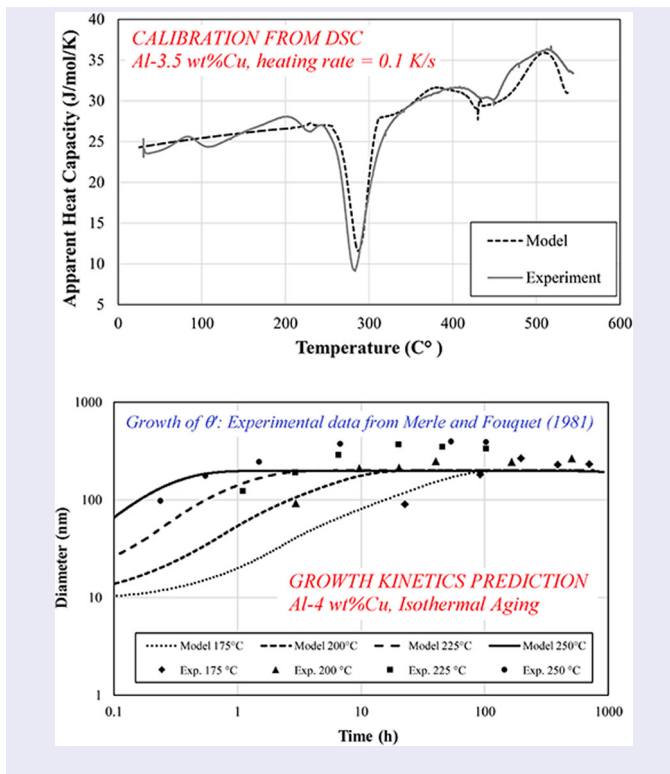
1. Introduction

The main purpose of modelling precipitation kinetics is twofold. The first one is the prediction of material properties and the second one is to provide a better understanding of phase transformations. Contrary to models trying to visualise the complexity of the evolution of a population of precipitates in a 3D domain, which can hardly be predictive because of their inherent complexity, precipitation kinetics models based on the analytical solution of the mass conservation equation should have some predictive value, otherwise one may consider that they have a limited interest because of the important simplifications made to have an efficient computational scheme. The need for predictability is driven by the industry, which cannot rely on models working with a too large set of fitting parameters. Among the factors limiting the predictability of models comes first the nucleation of precipitates. Application of the classical nucleation theory (CNT) in solid-state transformation brings a lot of assumptions relative to the interfacial energy and the influence of defects. It is difficult with this theory to predict correctly the apparition of the most stable phases and why they seem to form at higher temperatures or much later in the process. To fit the observations, one has to adjust the value of the interfacial energy and the number of active sites where nucleation is possible.

Some researchers have investigated the kinetics of precipitation by adjusting the interfacial energy to explain the heat flow evolution measured during a differential scanning calorimetric (DSC) measurement. Among them, Khan et al. [1] used two different values of the interfacial energy; one for nucleation and another one for coarsening to model the isothermal precipitation kinetics in an Al-Cu-Mg alloy. They cited Robson et al. [2], who wrote that 'the interfacial energy measured for coarsening is too large to give a reasonable nucleation rate, and the interfacial energy for nucleation is too small to give the correct coarsening behavior'. For isochronal DSC measurements, Khan and Starink [3] used a temperature-dependent evolution of the interfacial energy and obtained a satisfactory agreement, except for the sharp endothermic peak generated by the change in interfacial energy imposed in the model after nucleation. This was considered as an artifact of the model that could be corrected by adapting the temperature evolution of the interfacial energy. On a similar alloy, Hersent et al. [4] used also a temperature-dependent value of the interfacial energy to obtain a reasonable fit between the heat flow calculated with their model and the heat flow measured by DSC. These authors applied the model of Myhr and Grong [5] for nucleation, growth, and dissolution of the S precipitates and mentioned that changing the interfacial energy by 10% produces a change in peak temperature of about 100 K. This was revealing the quasi impossibility of predicting precipitation kinetics during isochronal heating of alloys using an approach where nucleation rates are calculated by the CNT because of the too large impact given to the interfacial energy. Instead of calibrating the interfacial energy to mimic the DSC curve, Afshar et al. [6] used an incubation time that varies with temperature and time for each phase.

There are other approaches for studying precipitation like the thermo-kinetic model of MatCalc [7]. However, the accuracy of this method also depends noticeably on the exact parameter settings, like nucleation sites, dislocation density, degree of interface coherency, and so on. It should be noted that depending too much on fitting parameters weakens the predictability of kinetic models. But, even after fine-tuning the set of parameters, important deviations remain between calculated and measured DSC curves, especially at high temperatures [8–10]. One of the negative aspects of using adjustable parameters for the nucleation of precipitates is that it leads to discrepancies in the literature. For instance, Huis et al. [11] reported the volumetric mismatch between β'' and Al−Mg−Si matrix as 9.8%, but, Falahati et al. [8] used 2.5% to get a better fit. As another example, Afshar et al. [6] considered the density of dislocation as 1×10^{10} $(1/m^2)$, while Falahati et al. [8] used 1×10^{11} $(1/m^2)$ for similar Al-Mg-Si alloys.

It is mentioned that one of the obstacles against the prediction and validation capabilities of kinetic models is the fine-tuning of the interfacial energy. The issue of the interfacial energy, which acts as a limiting factor in the kinetic models, has been criticised by the subcritical growth theory [12]. According to

this theory, embryos can be divided into losers and winners. The winner particles can grow at the expense of the dissolution of the losers, the growth rate of the formers being not limited by the capillarity force. This concept of winners and losers is not different from the one derived from the CNT. Indeed, according to the CNT, the steady-state nucleation rate is given by the following expression [13]:

$$\frac{dN}{dt} = N_0 Z \, \beta \exp\left(\frac{-\Delta G^*}{kT}\right)$$ (1)

where the exponential term represents the probability of an embryo to reach the critical size. Multiplying this exponential by the Zeldovich factor (Z) gives the probability that the embryos having the critical size belong to the winners. The number density of winners depends therefore largely on the interfacial energy via these terms. The subcritical growth theory tells that the frequency factor (β) represents the growth rate of the winners, the latter being not influenced by the interfacial energy. This means that in situations where the precipitation kinetics is controlled by the growth process, it should be possible to predict the growth rates of the winners during and after the nucleation process.

Up to now, the role of the interfacial mobility has been neglected in the vast majority of models proposed in the literature. The reason is that precipitation kinetics is assumed to be essentially diffusion-controlled. But ignoring the dissipation of energy at the interface (or ignoring the role of the interfacial mobility) in the diffusion-control approach is only a simplification, phase transformations occurring usually under a mixed-mode regime [14,15]. In this regard, Larouche [16] showed that considering the interfacial mobility as a variable in the kinetic model leads to different interface velocity particularly in the early stage of the evolution. That model provided a quasi-stationary solution for a precipitate in an infinite binary matrix [16]. This approach was extended for the growth of multicomponent precipitates [17], and a time-discretization technique was introduced to upgrade the analysis capability of the model for finite systems, including the dissolution of the unstable phases [18]. Nevertheless, the application of all these contributions [16–18] was limited so far to the isothermal evolution of only one type of precipitate. In the current contribution, the goal is upgrading our previous model to apply it for non-isothermal cases and with more than one type of precipitates. To reach this goal, the interfacial mobility values, which were recently reported by our research team [19], will be used and adjusted. Also, verification of the model will be done both with experimental DSC thermograms as well as the size evolution of precipitates measured independently by other researchers.

2. Methodology

2.1. Initial conditions during the subcritical growth regime

Continuous precipitation occurs in general at low supersaturation, for instance when a slow cooling rate is imposed after homogenisation. But after a rapid quench at room temperature, the assumption about nucleation sites saturation is generally accepted [20]. The growth model presented below will be applied for the case where a binary system has been solutionized and quenched to obtain a fully supersaturated solution. We will consequently assume that precipitation kinetics is controlled by the growth process. The number of precipitates per unit volume N_ϕ of each phase ϕ obtained after the quench will correspond to the number density of the winners according to the subcritical growth theory. This number density will be set constant for the entire growth regime. All phases are assumed to compete with each other right after the quench. The mixed-mode model will start only once the ellipsoidal precipitate reaches a critical size $a_1 = a_c$ after a time $t = t_c$. Before this time, growth is interface-controlled, and it is assumed that the precipitates are all spherical at time 0. Their evolution between time 0 and t_c depends on the equilibrium shape they are supposed to get at time t_c. Notice that a_1 is defined as the longest semi-axis length of the ellipsoidal precipitate. During the interface-controlled regime, the growth velocity is calculated with the following equation [12]:

$$\frac{\mathrm{d}a_1}{\mathrm{d}t} = v_c = \frac{MRT}{V_m} \sum_{i=1}^{I} c_\phi \cdot \ln\left(\frac{\bar{c}}{c_{eq}^\infty}\right) \tag{2}$$

where c_ϕ is the solute molar fraction of the precipitate, $\bar{c}$ is the average molar fraction of solute in the matrix, c_{eq}^∞ is the equilibrium molar fraction of solute in the matrix according to the phase diagram, M (m^4 J^{-1} s^{-1}) is the mobility of the interface at the tip of the precipitate, R (J mol^{-1} K^{-1}) is the gas constant, V_m (m^3 mol^{-1}) is the molar volume of the precipitate and T (K) is the absolute temperature. The critical velocity v_c represents the maximum interfacial velocity possible in a matrix having an average composition $\bar{c}$. It is the growth velocity of the winners according to the subcritical growth theory. It is why v_c is not impacted by the Gibbs-Thomson effect, as is the case for the frequency factor in the CNT. Notice that the strain energy is ignored in Equation (2), or is assumed to be accounted for by the phase diagram. During the interface-controlled mode, the geometry of the precipitates is assumed to change gradually from spherical to ellipsoidal according to the aspect ratio found by the experiments. For a disk-shaped precipitate, the radius of the disk is supposed to grow, while the thickness remains constant up to the beginning of the mixed-mode

regime. Notice that Equation (2) will also be used when a dissolving precipitate will reach its critical size. In such a case, $c_{eq}^{\infty} > \bar{c}$, and the velocity of the interface is negative. Here also, the shape of the dissolving precipitate will be assumed to change gradually and becomes spherical as the size will be decreasing down to zero.

2.2. Evolution equations for the mixed-mode regime

The mixed-mode model for the evolution of an ellipsoidal precipitate in a binary infinite matrix has already been reported in our previous contributions ([16]: Growth model), and ([18]: Dissolution model). During the mixed-mode regime, it is assumed that the precipitates evolve with a constant aspect ratio. Accordingly, the following equation should be solved for the growth model [16] to obtain a_1 for a given time t:

$$\frac{\bar{c} - c^*}{c_\phi - c^*} = \frac{a_1^3 \sqrt{1 - e_{12}^2} \sqrt{1 - e_{13}^2}}{2D \cdot t} \exp\left(\frac{a_1^2}{4D \cdot t}\right)$$
$$\times \int_{a_1}^{\infty} \left[(\rho^2 - e_{12}^2 a_1^2)^{-1/2} (\rho^2 - e_{13}^2 a_1^2)^{-1/2} \exp\left(-\frac{\rho^2}{4D \cdot t}\right) \right] d\rho \quad (3)$$

where c^* is the solute molar fraction of the matrix at the interface, and D is the coefficient of diffusion of the solute in the matrix. The parameters e_{12} and e_{13} are the ellipsoidal eccentricities defined as:

$$e_{12} = \sqrt{1 - (a_2/a_1)^2} \quad (4)$$

$$e_{31} = \sqrt{1 - (a_3/a_1)^2} \quad (5)$$

where a_2 and a_3 are the two other principal semi-axis lengths ($a_1 \geq a_2 \geq a_3$). The particularity of the Larouche analytical solution for the mixed-mode case is to provide an equation linking c^* to the chemical driving force, the mobility of the interface M, and the interfacial energy γ_1, the latter being defined where the ellipsoid has its smallest radius of curvature. The following expression was obtained:

$$c^* = c_{eq}^{\infty} \exp\left(\frac{V_m \cdot a_1}{2c_\phi MRT \cdot k_g t^{3/2}} + \frac{2V_m \gamma_1}{c_\phi RT a_1}\right) \quad (6)$$

where k_g is the interface migration coefficient for growth, which is given by:

$$k_g = \frac{1}{2}\sqrt{\frac{v_c}{a_c}} \quad (7)$$

Similarly, the equations for the dissolution under the mixed-mode regime

(reversed-growth approximation) are expressed as [18]:

$$\frac{c^* - \bar{c}}{c_\phi - c^*} = \frac{a_1^3 \sqrt{1 - e_{12}^2} \sqrt{1 - e_{31}^2}}{2D \cdot \tau} \exp\left(\frac{a_1^2}{4D \cdot \tau}\right)$$

$$\times \int_{a_1}^{\infty} \left[(\rho^2 - e_{12}^2 a_1^2)^{-1/2} (\rho^2 - e_{31}^2 a_1^2)^{-1/2} \exp\left(-\frac{\rho^2}{4D \cdot \tau}\right) \right] d\rho \quad (8)$$

$$c^* = c_{eq}^{\infty} \exp\left(\frac{-V_m \cdot a_1}{2c_\phi MRT \cdot k_d \tau^{3/2}} + \frac{2V_m \gamma_1}{c_\phi RT a_1}\right) \quad (9)$$

where τ is the time remaining before complete dissolution. The interface migration coefficient for dissolution k_d is the same as for growth except that v_c is replaced by $-v_c$, so that a positive value is obtained inside the square root. As for growth, a_c is the size below which the boundary migration is interface-controlled. Notice however that the values of a_c for growth and dissolution can differ, but will be assumed equal in both regimes.

2.3. Upgrading the size of precipitates and the average composition of the matrix

Since non-isothermal precipitation is considered in this paper, the temperature-dependent parameters (c_{eq}^{∞}, M and D) must be updated at each time step. Also, to transform the solution from a quasi-stationary case where $\bar{c}$ is constant, into a finite system where $\bar{c}$ changes gradually with time, the time discretization technique presented in our previous contribution [18] must be used to calculate the growth velocity $\partial a_1/\partial t|_{\bar{c}(t)}$ at each time step. The size of the precipitates is then calculated with the following equation:

$$a_1(t + \Delta t) \approx a_1(t) + \left.\frac{\partial a_1}{\partial t}\right|_{\bar{c}(t)} \Delta t \quad (10)$$

Considering a one-size distribution of ellipsoidal precipitates, the volume fraction g_ϕ of each phase ϕ is simply given by:

$$g_\phi = N_\phi \cdot \frac{4}{3} \pi a_1 a_2 a_3 \quad (11)$$

The upgraded composition of the matrix can then be calculated with the following equation:

$$\bar{c} = \frac{c_0 - \sum_{\phi=2}^{N} g_\phi c_\phi}{\left(1 - \sum_{\phi=2}^{N} g_\phi\right)} \quad (12)$$

where c_0 is the nominal composition of the system and N is the number of phases involved. The index $\phi = 1$ refers to the matrix. The flowchart of the growth and dissolution behaviour of the multiphase system is presented in Figure 1.

To facilitate the reading of the flowchart, a brief explanation is presented. The precipitates are assumed to grow or dissolve in a cell where the only active phases are the matrix and the precipitate. Since the precipitates have different interfacial mobility and chemical driving force, they will have different growth rates. For example, precipitate $\phi = 2$ can reach the mixed-mode region sooner than precipitate $\phi = 3$. The other important difference between them is that the equilibrium concentrations with the matrix are different. Suppose that $c^{\infty}_{eq, \phi=2} > c^{\infty}_{eq, \phi=3}$; then as soon as $\bar{c}$ is getting lower than $c^{\infty}_{eq,\phi=2}$, precipitates of phase $\phi = 2$ start to dissolve while precipitates of phase $\phi = 3$ continue to
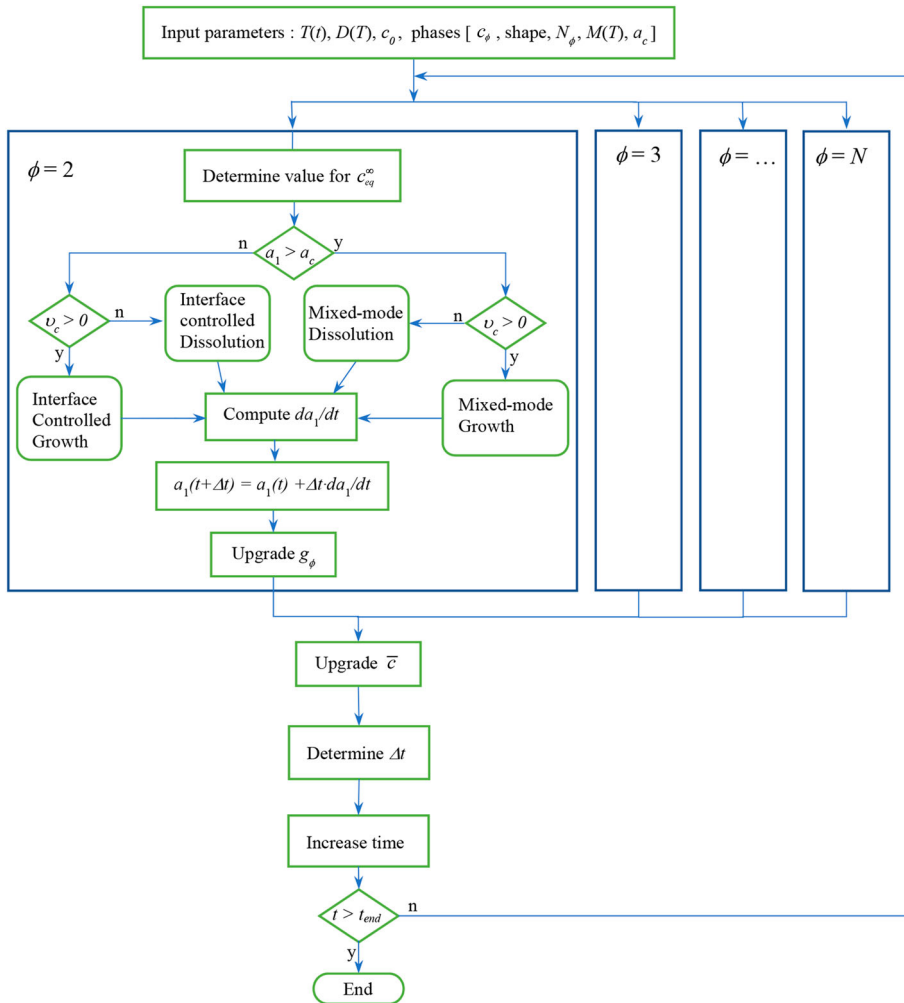

Figure 1. Schematic of the growth and dissolution model for the multiphase system.

grow. The calculation of υ_c allows us to know if the precipitate is growing or dissolving.

For the simplification purpose, the number densities of precipitates are assumed constant in the model. This assumption is acceptable beyond the initial stage of growth because the concentration gradient isolates each precipitate preventing the ripening phenomenon. As an example, one can find stability in the number density of precipitate during the growth region in reference [6]. Of course, the number density is changing during the subcritical growth regime under the circumstances that the concentration gradient in the matrix is negligible and ripening occurs. Since the embryos remain very small during this stage, taking into account the rise and fall of the losers does not push any noticeable variation in terms of the latent heat released. Late ripening occurring when the volume fraction of precipitates reach a quasi-equilibrium state is also not taken into account in this model.

2.4. Using the model to depict the DSC thermograms

To compare the model's results with the DSC thermograms, the temperature derivative of the enthalpy of the system must be calculated. Using MatCalc [7], one can obtain the molar enthalpy h_ϕ of the phases at a given temperature and composition. Since the molar volume is assumed the same for all phases, the molar enthalpy of the system can be calculated with the following equation:

$$h = \sum_{\phi=1}^{N} g_\phi \cdot h_\phi \tag{13}$$

The apparent heat capacity is obtained by calculating the derivative of the system enthalpy with respect to temperature.

2.5. Application of the model

The model will be applied to calculate the size evolution of precipitates in two alloys submitted to different aging conditions. The first one is the Al-3.5 wt% Cu used by Heugue et al. [19], who investigated the growth kinetics of precipitates in this alloy during isochronal DSC analysis. The second alloy is the Al-4 wt% Cu used by Merle and Fouquet [21] in their investigation of isothermal coarsening of θ' after a short reversion treatment.

For the DSC comparison, three different types of precipitates (θ'', θ', and θ) are considered in the model. These precipitates are characterised by the parameters given in Table 1. Most of these parameters were determined based on the works of Heugue et al. [19] who have studied the alloy used in the present contribution. The values for the number density and aspect ratio were adjusted to obtain a better fit with the DSC results. The initial value of a_1 at the start of the simulation

Table 1. Parameters used for the simulation of aging for the Al-3.5 wt%Cu alloy.

	θ''	θ'	θ
Chemical composition	Al$_3$Cu	Al$_2$Cu	Al$_2$Cu
Number density of precipitate, N_ϕ (m^{-3})	1.4×10^{22}	3.0×10^{20}	2.0×10^{18}
Initial value of a_1 at the start of the simulation (nm)	0.4	0.4	0.4
Semi-axis length at the start of mixed-mode, a_c (nm)	5	20	20
Aspect ratio at the start of mixed-mode (oblate spheroids)	20	25	15

corresponds roughly to the unit cell size of the FCC matrix. This value has a very limited impact on the results. The semi-axis length at the start of mixed-mode, a_c was first chosen according to the expected aspect ratio and precipitates thicknesses for Al-Cu precipitates starting to grow in an aluminum matrix, the thickness ranging between 1- or 3-unit cells of the FCC matrix. The values for a_c were adjusted manually and those giving the better fit are given in Table 1. The coefficient of diffusion of Cu in Al and the equilibrium molar fraction relevant to each secondary phases were determined from the MatCalc software application using the databases assessed by Povoden-Karadeniz [22,23]. The interfacial mobility was calculated with the following expression:

$$M = \frac{\Omega}{RT} \exp\left(-\frac{E}{RT}\right) \tag{14}$$

where Ω and E were optimised according to the DSC curves. Values determined by Heugue et al. [19] were used as initial trial values. It was found that different constant values of Ω and E for growth and dissolution had to be set for a good fitting, except for the θ'' phase, for which the same value of interfacial mobility was used for growth and dissolution.

For the second alloy, the same set of parameters was used for the precipitates to evaluate the predictive capability of the growth model.

All calculations were made by assigning a zero value to the interfacial energy on the basis that this variable does not impact the growth rate of the winners during the subcritical growth regime, and has a limited impact on the growth regime.

3. Results

The main concept of the mixed-mode approach is to considering interfacial mobility as an effective variable in the early stage of growth, but also on the late stage of dissolution. The final values for Ω and E obtained by fitting the model with the DSC isochronal heating curves are presented in Table 2, and the obtained evolutions of interfacial mobility versus temperature are presented in Figure 2.

The temperature evolutions of the interfacial mobility used in the model are compared with those determined by Heugue et al. [19] according to their Kissinger analysis (curves with symbols '+', and '×'). One can see that the agreement

Table 2. Optimised values for Ω and E in the expression calculating the interfacial mobility.

Phases	Growth		Dissolution	
	Ω (m⁴/mol/s)	E (kJ/mol)	Ω (m⁴/mol/s)	E (kJ/mol)
θ″	7.208E-02	123.9	7.208E-02	123.9
θ′	9.636E-05	111.1	1.508E+01	198.6
θ	9.882E+13	316.4	1.459E+06	298.9

is excellent for the growth of the θ′ phase but a substantial difference is obtained for the growth of the θ phase. The comparison between the apparent heat capacity calculated by the model and measured by the DSC for a heating rate of 6 K/min is presented in Figure 3. Notice that the DSC curve is the same as the one obtained by Heugue et al. [19], except that only the instrumental baseline was subtracted from the DSC curve, keeping thus the variation of the heat capacity with temperature. The experimental curve was shifted vertically so that the apparent heat capacity at low temperatures fits the apparent heat capacity determined by MatCalc. Heugue et al.[19] had flattened the baseline curve to a straight line to facilitate the determination of peak temperatures, but this operation was removing the variation of the heat capacity with temperature.
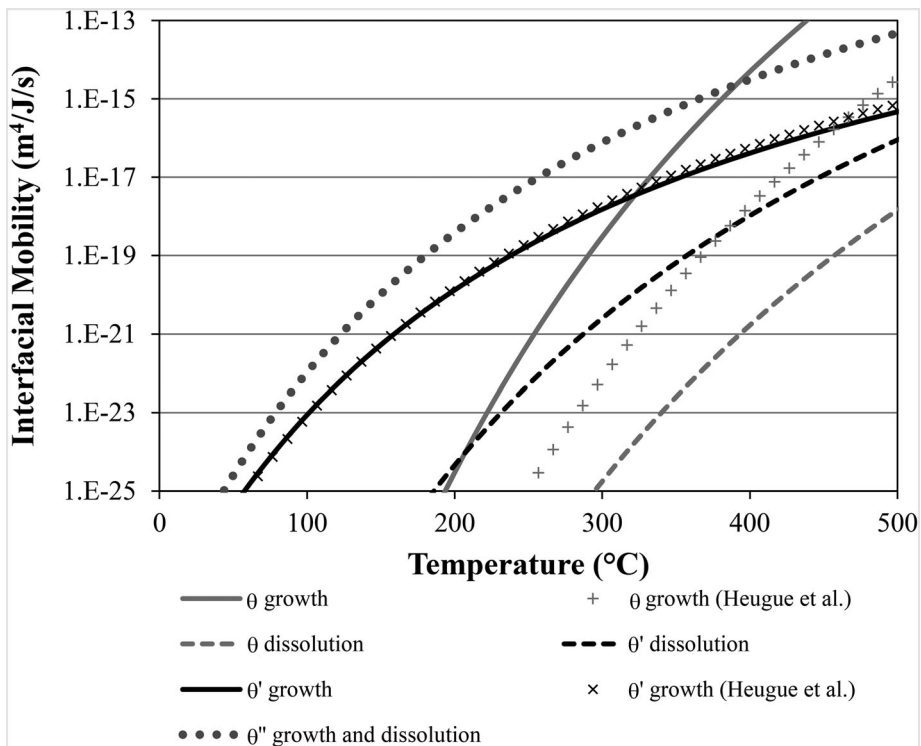
Figure 2. Evolution of the interfacial mobility of precipitates versus temperature evaluated in the Al-3.5 wt%Cu alloy.
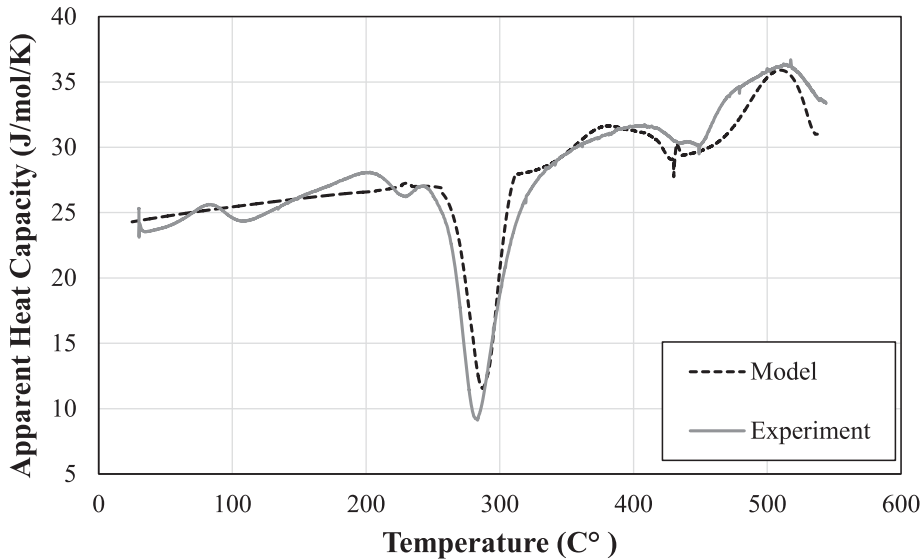
Figure 3. Comparison between the apparent heat capacity calculated by the model and measured experimentally during the decomposition of the supersaturated Al-3.5 wt%Cu alloy occurring with a heating rate of 6 K/min. The experimental curve was retrieved from the work of Heugue et al. [19].

The size and volume fraction evolutions of the precipitates giving the theoretical apparent heat capacity curve presented above are plotted in Figure 4.

The maximum size of precipitates depends on their number density; it is why the θ' precipitates reach a lower plateau than the θ precipitates, but a higher plateau than the θ'' precipitates. The peak volume fraction depends almost entirely on the Cu solubility of the matrix c_{eq}^{∞}. When the latter is high, the maximum volume fraction is low. The peak volume fraction of the precipitates is therefore related to the fact that c_{eq}^{∞} for θ'' is very high at low temperatures, high for θ at high temperatures and low for θ' at intermediate temperatures. Notice that the coexistence of phases θ' and θ in the matrix predicted by the model was observed by Heugue et al. [19] on the same alloy after isothermal aging of 6 and 12 h at 190°C. The 3 solvus curves determined with MatCalc are plotted in Figure 5, as well as the theoretical curve showing the evolution of $\bar{c}$ as the temperature was increasing. For each type of precipitate, growth is expected as long as $\bar{c}$ is larger than the solubility of the matrix at a given temperature. When $\bar{c}$ crosses the solvus upon heating, the dissolution of the precipitate begins.

The good agreement between the DSC curves and the model was obtained because of the possibility to fine-tune the value of Ω, E of the interfacial mobility and the number density N_{ϕ} of the different types of precipitates. The values for N_{ϕ} used in the model were close to the values determined by Heugue et al. [19]. They differ slightly but remains inside a realistic margin. The same reasoning
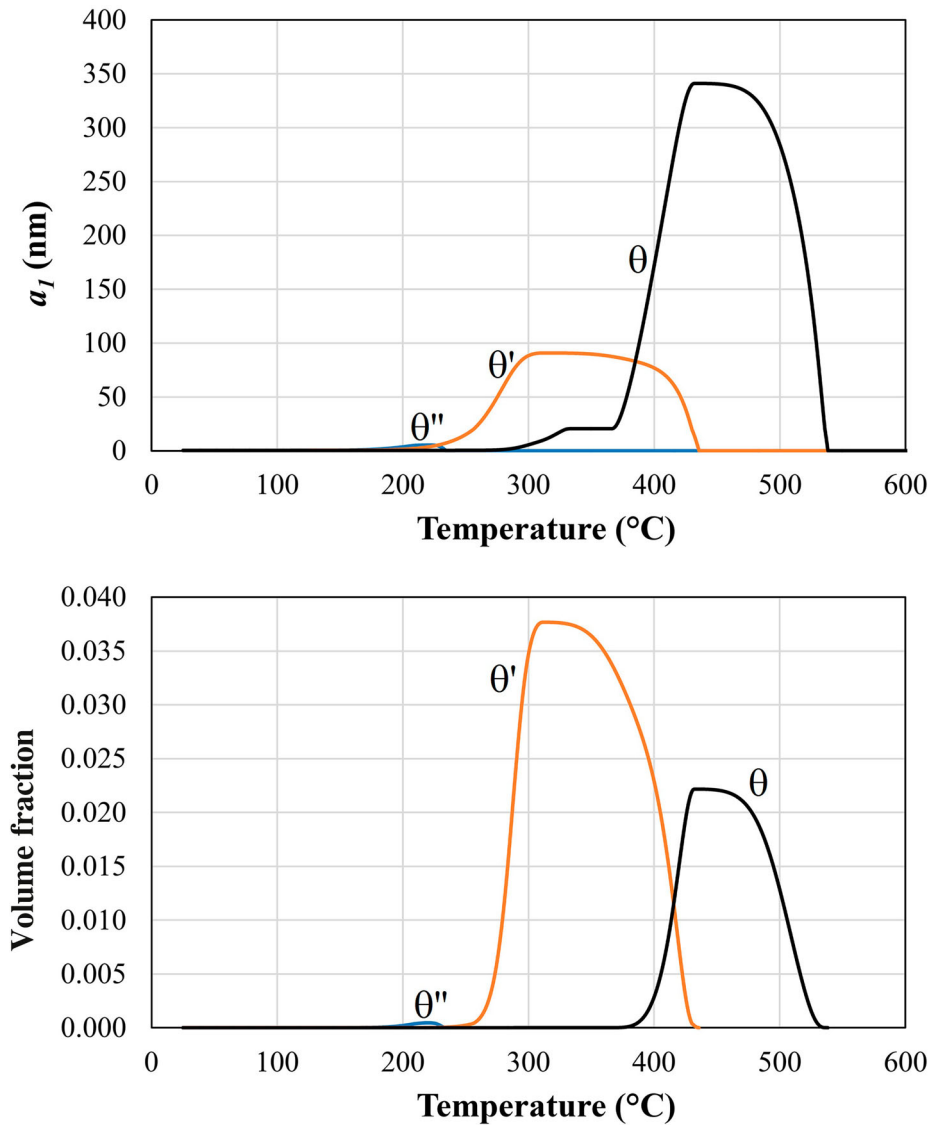
Figure 4. Calculated evolution of the size (a_1) and volume fraction of the precipitates versus temperature during the decomposition of the supersaturated Al-3.5 wt%Cu alloy occurring with a heating rate of 6 K/min.

was applied for the activation energies, where a reasonable agreement with the Kissinger analysis had to be maintained. In the narrow margin of the possible values for Ω, E and N_ϕ, our model was suitable to reproduce the DSC curves. For comparison purposes, it is interesting to look at the results given by the model if one assumes that growth is diffusion controlled. This can easily be done by giving a very high value to the interfacial mobilities, as well as assigning a very small value to a_c. Figures 6 and 7 present the evolution curves obtained using the same number densities as in the previous simulation. As expected,
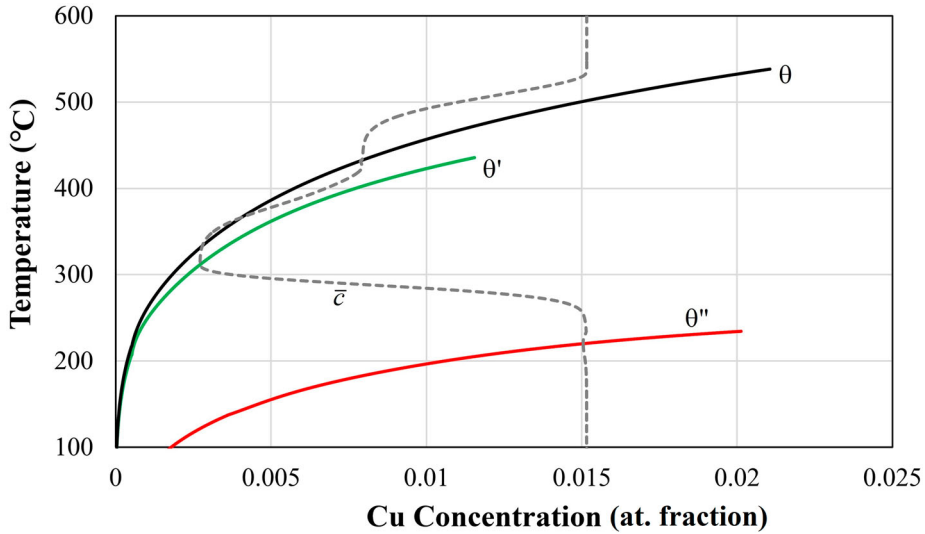
Figure 5. Evolution with the temperature of the θ″, θ′, and θ solvus as determined by MatCalc, and of the Cu solute molar fraction of the matrix ($\bar{c}$) as calculated by the model for the decomposition of the supersaturated Al-3.5 wt%Cu alloy occurring with a heating rate of 6 K/min.

all precipitates start to grow simultaneously at very low temperatures, the growth rate of θ and θ′ being close to each other in the acceleration stage. Such behaviour in the precipitation kinetics of these two phases is not the one expected in Al-Cu alloys prepared under similar conditions. The shallow intense peak starting at 400°C results from the too rapid transformation kinetics of θ and θ′ precipitates, which are not limited by their interfacial mobility. The agreement with
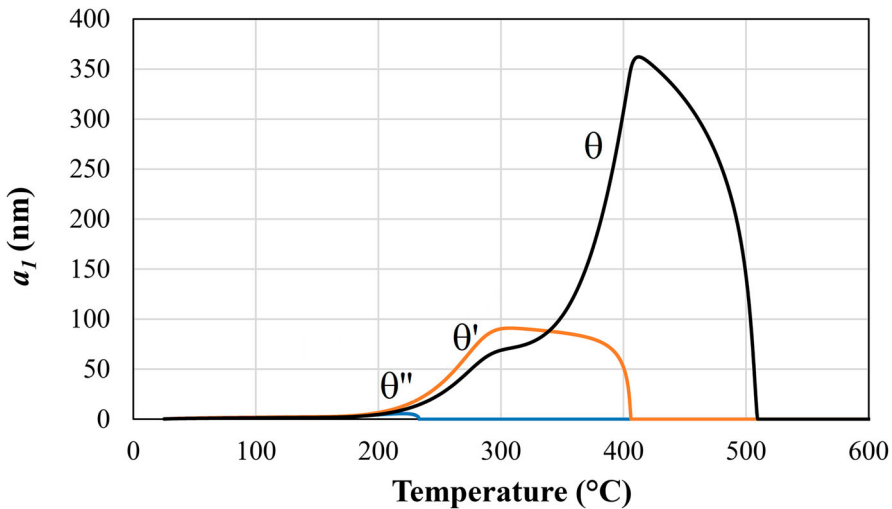

Figure 6. Calculated diffusion-controlled evolution of the size (a_1) of the precipitates during the decomposition of the supersaturated Al-3.5 wt%Cu alloy occurring with a heating rate of 6 K/min.
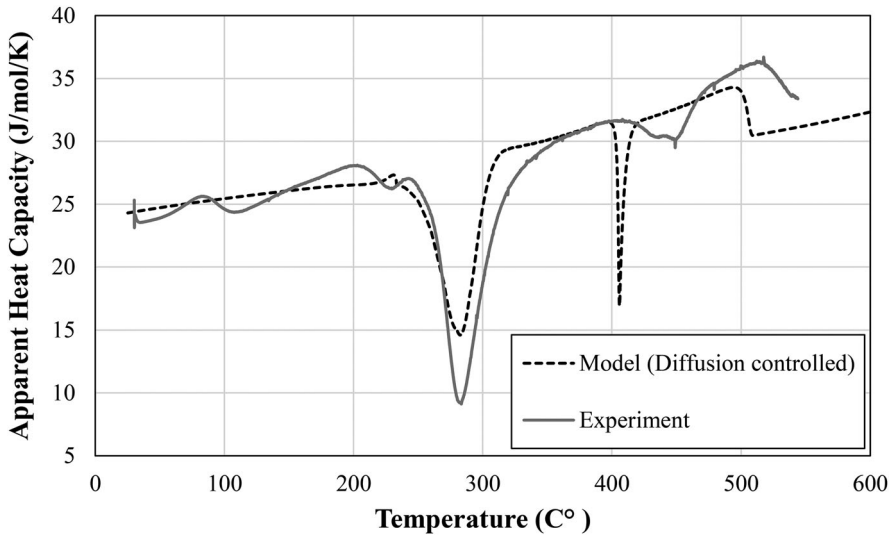
Figure 7. Comparison between the apparent heat capacity calculated by the model with diffusion-controlled kinetics and the apparent heat capacity measured experimentally during the decomposition of the supersaturated Al-3.5wt%Cu alloy occurring with a heating rate of 6 K/min. The experimental curve was retrieved from the work of Heugue et al. [19].

the experimental curve is for that reason less satisfactory than with the mixed-mode model.

Despite the flexibility given by the interfacial mobilities, the DSC peak associated with the θ phase was difficult to reproduce with the mixed-mode model because of the concomitant growth of the θ phase and the dissolution of the θ′ phase. The simultaneity of these phase transformations was responsible for the relatively low amplitude of that peak. As one can see in Figure 5, the calculated transformation path is such that $\bar{c}$ evolves by staying close to the solvus of the θ phase between 330 and 430°C. Indeed, $\bar{c}$ crosses that solvus three times during the scan, which explains the irregular shape of the peak. This behaviour explains also why the interfacial mobility curve used for the growth of the θ phase differs significantly from the one determined by Heugue et al. [19]. The previous analysis made to determine the kinetic parameters of the θ phase was not taking into account the dissolution of the θ′ precipitates. Considering the present model, one can conclude that the factor limiting the growth rate of the θ precipitates above 370°C was the dissolution rate of the θ′ precipitates. Notice that the activation energies for the growth of the θ phase are not so different between the two investigations. The difference is essentially caused by the pre-exponential factor Ω.

The evolution of the θ″ phase was almost 100% controlled by the interface and its volume fraction remains very low as explained above. The interfacial mobility used for the growth of θ″ precipitates allows a good prediction of the onset temperature for that phase during a DSC heating scan, but the

correspondence between the calculated and the measured peak amplitude is not so good. This is likely due to the data retrieved from the phase diagram, knowing that there is large uncertainty about the true solvus of θ'', the experimental data used to validate this solvus being scarce and approximate since they depend on the size of the precipitates [24]. For that reason, trying to get a better fit with the interfacial mobility during the dissolution of this phase was not attempted. Therefore, we have preferred to use the same interfacial mobility for dissolution and growth. For the 2 other types of precipitates, it is clear that the interfacial mobility between growth and dissolution must differ to obtain a good fit. Rodriguez-Veiga et al. [25] have already reported that the activation energies associated with the growth and dissolution of a precipitate are different in an Al-4 wt% Cu. In their study, the activation energy for dissolution of θ'' and θ' was larger than for growth.

Because the growth rates of the winners during the subcritical growth regime are strongly impacted by the interfacial mobility, phases with higher interfacial mobility grow at a high pace before phases having lower interfacial mobility during the heating scan. According to this theory, the onset temperatures in a DSC heating scan are not ruled by the multiplication of nuclei, but by the accelerated growth of the existing precipitates, which is in agreement with the statement that precipitation kinetics at low temperatures is controlled by growth. It is worth mentioning that according to the CNT, the subcritical growth regime is part of the nucleation process. So, it seems more appropriate to say that the onset temperatures are essentially related to the acceleration of the growth of the precipitates and not to the multiplication of nuclei at this temperature, the latter occurring very soon after the quench. Of course, new precipitates can appear in any stage of the aging process since nucleation is a probabilistic phenomenon driven by the chemical driving force and the generation of new interfaces. But the occurrence of late nucleation is rare in comparison with the dominating process giving birth to a large number of nuclei at the start when the chemical driving force is maximal.

Figure 8 shows the impact of the heating rate on the apparent heat capacity evolution. By applying different heating rates one can see a displacement in DSC peaks as expected [19]. Indeed, by increasing the heating rate, a small shift to the right side is observable because of the activation energy associated with the interfacial mobility. This is another indicator that confirms the correctness of the model.

So far, the capability of the model to reproduce the DSC thermogram has been discussed. The parameters associated with the mixed-mode model were assessed so now, one can make a step forward by verifying the predictability of the model. This will be done with the results coming from an independent experiment performed by Merle and Fouquet [21] with the second alloy mentioned before. The model was applied so that the reversion treatment was done first, followed by the isothermal aging at different temperatures. Figure 9
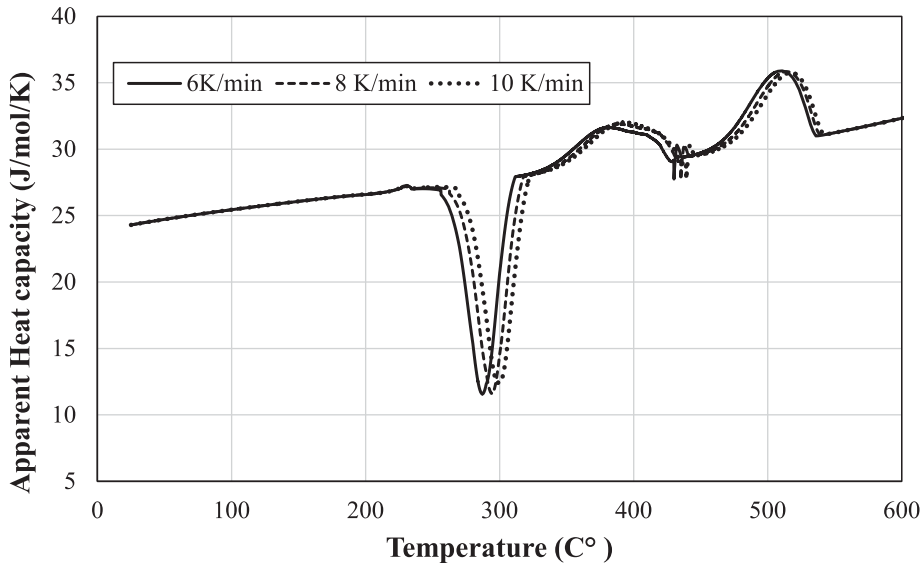
Figure 8. Influence of heating rate on the apparent heat capacity during the decomposition of the supersaturated Al-3.5 wt%Cu alloy.

shows the evolution of the diameter ($2a_1$) of the disk-shaped θ' as calculated by the model and measured by Merle and Fouquet. A very good agreement is achieved in terms of the average growth rate calculated at different temperatures
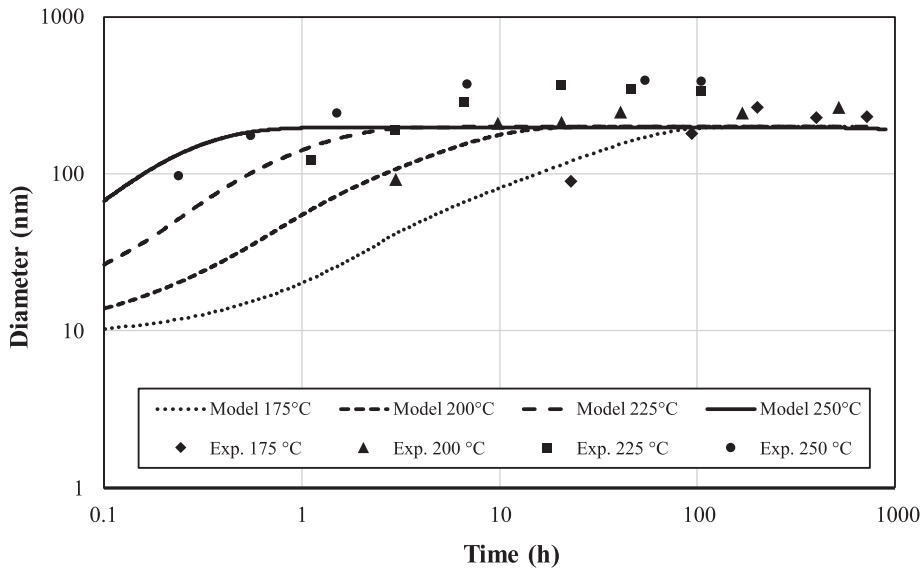

Figure 9. Evolution of the calculated and measured diameter of disk-shaped θ' precipitates in an Al-4 wt%Cu alloy submitted to a reversion treatment (3 min at 225°C) after the homogenisation and quench treatments. The number density of precipitates was the same for all temperatures. Experimental data were taken from reference [21].

for the first portion of the growth regime. A better fit of the maximum diameter can be obtained if one adjusts the number density of precipitates according to mass conservation, which gives the plots presented in Figure 10. It would have been easy to adjust slightly Ω and E to have a better fit of the growth rates measured by Merle and Fouquet, taking into account the fact that the nominal composition in Cu is not the same in the two alloys, but we thought preferable to present a raw prediction obtained after a calibration of the interfacial mobilities with the help of a DSC thermogram. Applying mass conservation imposed that the final volume fraction of the θ' precipitates measured from the experimental data corresponds to the volume fraction predicted by the phase diagram. Indeed, when the reaction is almost finished, one expects that the volume fraction of precipitates is close to the equilibrium value. If we know the average size and shape of the precipitates from the measurements, one can estimate their number densities accurately with the following equation:

$$\text{Vol. fraction at equilibrium} = \text{Number density} \cdot \left(\frac{4}{3}\pi a_1 a_2 a_3\right)_{\text{end of growth}} \tag{15}$$

For that matter, N_ϕ values of 2.7×10^{20}, 1.8×10^{20}, 1.0×10^{20}, and 7.0×10^{19} particles/m³ were determined respectively for isothermal aging at 175°C, 200°C, 225°C, and 250°C. These numbers were used to plot the curves presented in Figure 10. The number density used for the DSC analysis was 3.0×10^{20}. Such
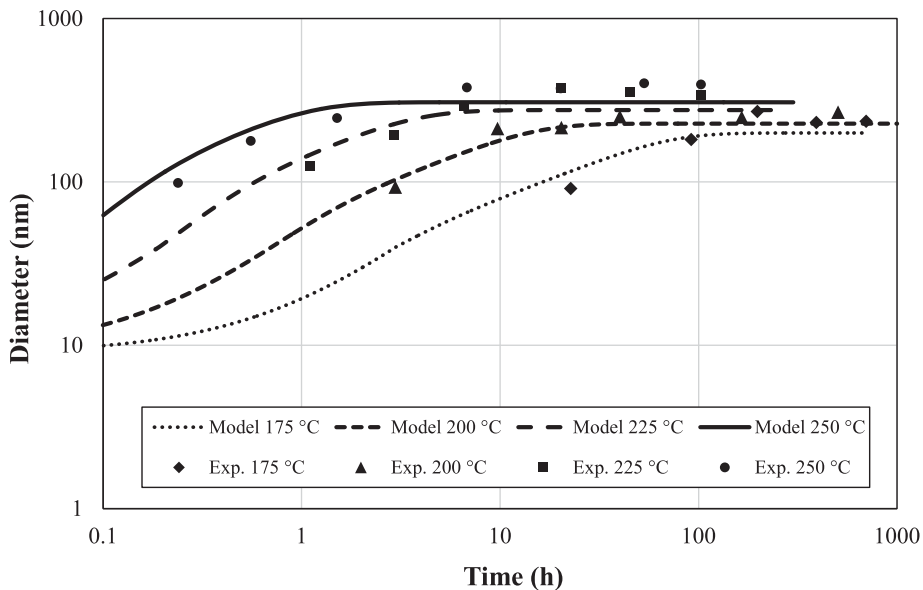

Figure 10. Evolution of the calculated and measured diameter of disk-shaped θ' precipitates in an Al-4 wt%Cu alloy submitted to a reversion treatment (3 min at 225°C) after the homogenisation and quench treatments. The number density of precipitates was adjusted for each temperature. Experimental data were taken from reference [21].

a slight difference is normal considering that the number density of precipitates depends on parameters like the nominal composition, the quench rate, the level of impurities, the grain size, the density of dislocations, and many other factors influencing the activation of nucleation sites.

4. Discussion

Even though the proposed model has few adjustable parameters, it was possible to reproduce correctly the DSC curves and the evolution of the size of the θ' precipitates made at 4 different temperatures, both set of measurements being done independently on two different Al-Cu alloys. Such a good agreement between a model and two independent sets of experimental results obtained in the study of precipitation kinetics of two similar alloys has no precedent in the literature. Among the adjustable parameters, those associated with the interfacial mobility (Ω and E) are the most important for the fitting of the DSC curves, taking as granted the accuracy of the thermodynamic variables and the coefficient of diffusion retrieved from the databases used by the MatCalc application software.

The coefficient of diffusion D and the interfacial mobility M are the two variables limiting the growth and dissolution kinetics in our model. They act differently as this can be visualised in Figure 11. In this schematic configuration of atoms representing a region containing 2 phases separated by an interface
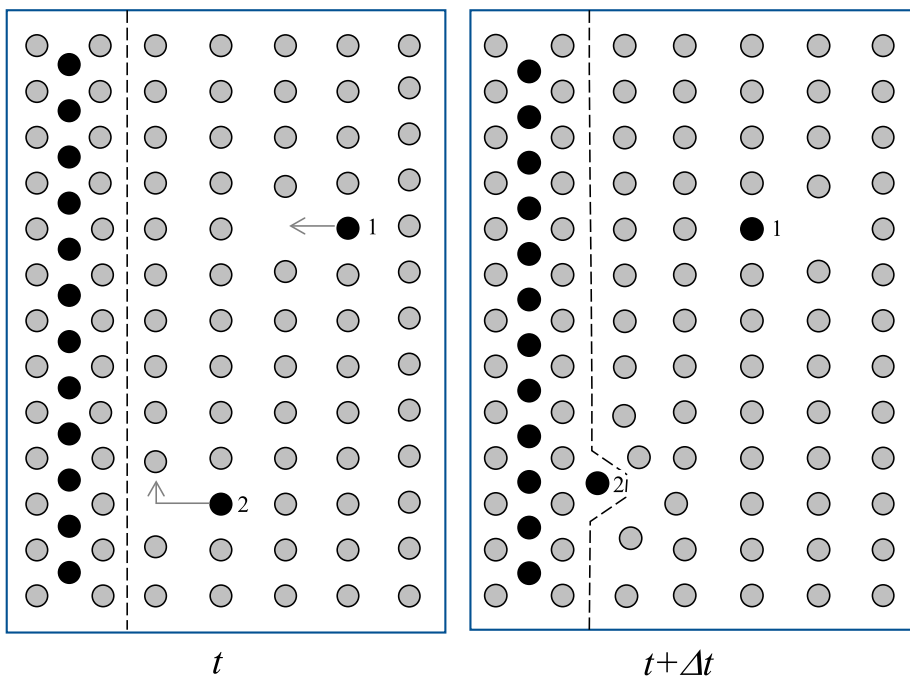

Figure 11. Schematic atomic configuration showing the difference between the diffusion (1) and the condensation (2) processes.

(the dotted lines), atom 1 migrates inside the matrix and the activation energy for this process is the one associated with diffusion. For atom 2, the local configuration of atoms is different at the interface from the one inside the matrix. The condensation of this atom is activated by kinetics associated with the interfacial mobility and one expects that the activation energy for this process differs from the one associated with diffusion in the matrix. Moreover, depending on the nature of the precipitates, the activation energy associated with the condensation of atoms depends on the nature of the precipitate, and probably on the elastic strain field surrounding it. It makes sense that the interfacial mobility and the processes related to it are important to describe the growth and dissolution of precipitates, especially when the precipitates are small and the diffusion fields not well developed around them.

The determination of Ω and E was difficult to achieve because of the high sensibility of the apparent heat capacity with the evolution of the volume fraction of the matrix versus temperature. Indeed, a discontinuity in the evolution of the volume fraction caused by the fitting procedure produces a step in the evolution of the apparent heat capacity, which is not related to a real event in the phase transformation process. This is why many authors accepted that their model produces unwanted peaks that they associated with numerical artifacts. Trying to fit a DSC curve is a very severe test for a precipitation model. It is why the values of the interfacial mobility and the evolution of volume fraction of the phases obtained with the proposed model can be considered as realistic and accurate. The other parameters used in the model (N_ϕ and a_c) can be adjusted, but only in a narrow margin and with a small influence on the results. The number density is a variable that can be easily determined experimentally and some numbers can be found in the literature. For instance, Heugue et al. [19] determined that the number density of the θ' precipitates was $(2.00 \pm 0.69) \times 10^{20}$ m^{-3} and $(1.73 \pm 0.46) \times 10^{20}$ m^{-3} after isothermal aging of respectively 6 and 12 h at 190°C. These values are close to the 2.7×10^{20} and 1.8×10^{20} m^{-3} values used at respectively 175 and 200°C in the modelling of the isothermal aging of Al-4 wt%Cu alloy. With the first alloy, a better fit of the amplitude of the DSC θ' peak was obtained with a number density of 3.0×10^{20} m^{-3}, which is also not far from the previous numbers. Of course, the alloys and the thermal history differ, and it seems that this had an impact on the number density. Ripening occurs and must be taken into account to have a better estimation of the number density of the precipitates, though its influence is not so important on the evolution of volume fraction and the apparent heat capacity. One exception is at high temperatures (above 450°C), where the model underestimates likely the dissolution rate of the θ precipitates. At very low temperatures, the process of ripening is also active and accelerates the rate of dissolution of clusters, GP zones, and other metastable precipitates. Since many phases were not considered and that ripening was not modelled, one could not expect to reproduce correctly the small bumps recorded at low

temperatures in the DSC curves. The last adjustable parameter was a_c. This variable sets the size beyond which the precipitate grows or dissolves in the mixed-mode regime. Setting $a_c = 0$ is equivalent to impose a diffusion-controlled regime, while setting $a_c = \infty$ is equivalent to impose an interface-controlled regime. Presently, there is no theory available to determine the criteria defining the size below which the phase transformation is interface-controlled. Larouche [12] assumed that this size should correspond to the moment where the number density of precipitates is almost stabilised. This critical size is not zero for sure nor infinite. A value for a_c ranging between 2 and 20 nm seems reasonable and one can see in Figure 12 that the impact of this variable in this range is marginal.

Aspect ratios were kept constant at reasonable values and the size distribution of each type of precipitates was kept monosized. In reality, the aspect ratios vary with time and the size distributions are not monosized. The impact of these variables is also small on the evolution of the volume fractions, but a more complex model including the role of the interfacial energy on the morphology and the ripening of the precipitates would allow to obtain smoother variations of the apparent heat capacity and likely a better fit with the DSC curves. The role of the interfacial energy has been completely evacuated in the model presented in this paper. The importance of this variable stands essentially on the value of the number density, the morphology, the size distribution, and the ripening phenomenon of the precipitates, all these factors having not been calculated or modelled. Contrary to the common idea that the interfacial energy rules
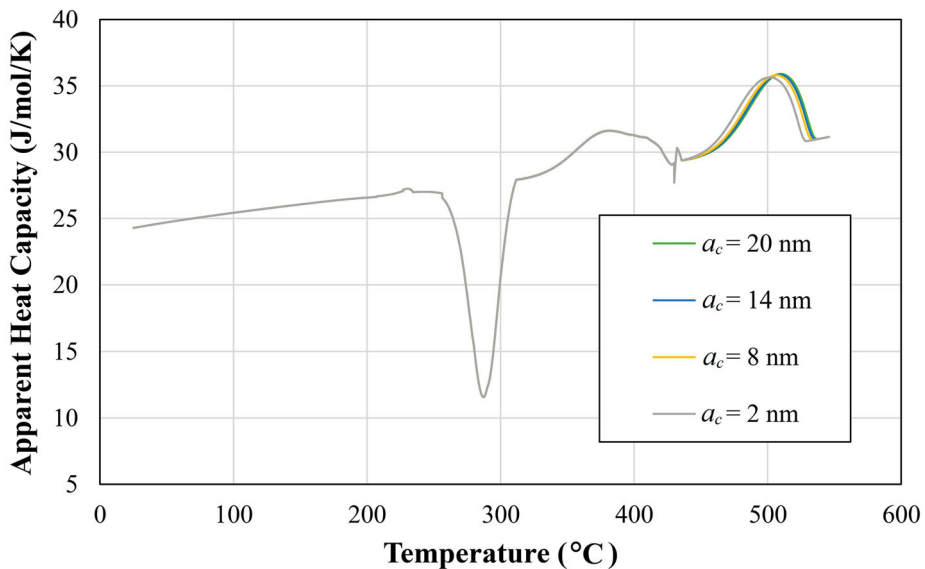

Figure 12. Influence of a_c value for θ phase on the calculated apparent heat capacity during the decomposition of the supersaturated Al-3.5 wt%Cu alloy occurring with a heating rate of 6 K/min.

the onset temperatures of the reactions or the incubation time, we have demonstrated that it is the interfacial mobility that has a direct impact on the onset temperatures obtained during the decomposition of supersaturated solutions. If one defines the incubation time for θ' precipitation as the time required for these precipitates to have a diameter of 30 nm, for instance, the model results indicate that the number density of precipitates has a marginal impact (< 0.1%) on the incubation time when the number density is less than 3.0×10^{20} m^{-3}. At this stage, the precipitates behave almost independently one from each other, which inevitably brings the early growth kinetics to be ruled by parameters like the interfacial mobility and mass diffusivities. This gives strong support to the subcritical growth theory, which tells that nucleation occurs in the interface-controlled regime and that the frequency factor of the CNT depends on the interfacial mobility. The interfacial energy is important in the process, but the way it varies with the size of the precipitates or with the temperature is likely not the best way to explain the sequence of precipitation.

5. Conclusion

In this research, a growth kinetic model has been developed to simulate non-isothermal heat treatments. Then, the validity and predictability of the model have been evaluated. For this purpose, the mixed-mode model was applied to simulate the kinetics pathway and sequence of precipitation in a binary Al-Cu alloy. The results obtained have been compared with experimental observations in terms of size evolution of the precipitates as well as the DSC thermograms. The results show that the mixed-mode model can accurately simulate the kinetic pathway of the precipitation. This progress in getting an accurate fit using the mixed-mode model sheds light on the worth of the interfacial mobility as an effective parameter in the kinetics of precipitation.

By applying the mixed-mode analytical solutions for the growth and dissolution of precipitates occurring during the aging of two Al-Cu alloys, we have shown that the kinetics of growth and dissolution in the context of a multiphase system can be accurately predicted if the interfacial mobility of all phases is known. To be fully predictive, the model should, however, include the role of the interfacial energy to predict the evolution of the number density of precipitates. We found that using reasonable values for the number density of precipitates was sufficient to obtain a good prediction of the evolution of the volume fraction and apparent heat capacity during the decomposition of a supersaturated system, even by considering a monosized distribution of the size of the precipitates. The task of predicting correctly the number density is very challenging, especially during the early stage of precipitation. Accurate modelling of precipitation kinetics will require more data on the evolution of the number density. The trend in past contributions in the field was to adjust the interfacial energy to fit the models with the experimental results. With the present contribution,

it is hoped that future developments will focus the role of the interfacial energy to the formation of subcritical nuclei at the very beginning of aging and how the number density of precipitates evolves with respect of time.

Disclosure statement

No potential conflict of interest was reported by the author(s).

References

[1] I.N. Khan, M.J. Starink and J.L. Yan, *A model for precipitation kinetics and strengthening in Al–Cu–Mg alloys.* Mater. Sci. Eng., A 472 (2008), pp. 66–74.

[2] J.D. Robson, M.J. Jones and P.B. Prangnell, *Extension of the N-model to predict competing homogeneous and heterogeneous precipitation in Al-Sc alloys.* Acta Mater. 51 (2003), pp. 1453–1468.

[3] I.N. Khan and M.J. Starink, *Microstructure and strength modelling of Al–Cu–Mg alloys during non-isothermal treatments: part 1 – controlled heating and cooling.* Mater. Sci. Technol. 24 (2008), pp. 1403–1410.

[4] E. Hersent, J.H. Driver and D. Piot, *Modelling differential scanning calorimetry curves of precipitation in Al–Cu–Mg.* Scripta Mater. 62 (2010), pp. 455–457.

[5] O.R. Myhr and Ø Grong, *Modelling of non-isothermal transformations in alloys containing a particle distribution.* Acta Mater. 48 (2000), pp. 1605–1615.

[6] M. Afshar, F. Mao, H. Jiang, V. Mohles, M. Schick, K. Hack, S. Korte-Kerzel and L.A. Barrales-Mora, *Modelling of differential scanning calorimetry heating curves for precipitation and dissolution in an Al-Mg-Si.* Comput. Mater. Sci. 158 (2019), pp. 235–242.

[7] E. Kozeschnik, MatCalc. Solid state and precipitation kinetics simulation software, 2012-07-02.

[8] A. Falahati, J. Wu, P. Lang, M.R. Ahmadi, E. Povoden-Karadeniz and E. Kozeschnik, *Assessment of parameters for precipitation simulation of heat treatable aluminum alloys using differential scanning calorimetry.* Trans. Nonferrous Met. Soc. China 24 (2014), pp. 2157–2167.

[9] P. Lang, T. Wojcik, E. Povoden-Karadeniz, A. Falahati and E. Kozeschnik, *Thermo-kinetic prediction of metastable and stable phase precipitation in Al–Zn–Mg series aluminium alloys during non-isothermal DSC analysis.* J. Alloys Compd. 609 (2014), pp. 129–136.

[10] E. Povoden-Karadeniz, P. Lang, P. Warczok, A. Falahati, W. Jun and E. Kozeschnik, *CALPHAD modeling of metastable phases in the Al–Mg–Si system*. Calphad 43 (2013), pp. 94–104.

[11] M.A. van Huis, J.H. Chen, M.H.F. Sluiter and H.W. Zandbergen, *Phase stability and structural features of matrix-embedded hardening precipitates in Al–Mg–Si alloys in the early stages of evolution*. Acta Mater. 55 (2007), pp. 2183–2199.

[12] D. Larouche, *A new theory of the solid-state growth of embryos during nucleation: the fundamental role of interfacial mobility*. Philos. Mag. 98 (2018), pp. 2035–2060.

[13] H.I. Aaronson, M. Enomoto and J.K. Lee, *Mechanisms of Diffusional Phase Transformations in Metals and Alloys*, Taylor & Francis, Boca Raton, 2010.

[14] G.P. Krielaart, J. Sietsma and S. Vanderzwaag, *Ferrite formation in Fe-C alloys during austenite decomposition under non-equilibrium interface conditions*. Mater. Sci. Eng., A 237 (1997), pp. 216–223.

[15] E. Kozeschnik, *Modeling Solid-State Precipitation*, Momentum Press, New York, 2013.

[16] D. Larouche, *Mixed mode growth of an ellipsoidal precipitate: Analytical solution for shape preserving growth in the quasi-stationary regime*. Acta Mater. 123 (2017), pp. 188–196.

[17] T. Naseri, D. Larouche, R. Martinez and F. Breton, *Mixed-mode growth of a multicomponent precipitate in the quasi-steady state regime*. Mater. Theory 2 (2018), pp. 1–14.

[18] T. Naseri, D. Larouche, R. Martinez, F. Breton and D. Massinon, *Analytical modeling of the mixed-mode growth and dissolution of precipitates in a finite system*. Metals. (Basel) 9 (2019), pp. 889.

[19] P. Heugue, D. Larouche, F. Breton, R. Martinez and X. Chen, *Evaluation of the growth kinetics of θ' and θ -Al$_2$Cu precipitates in a binary Al-3.5 Wt Pct Cu alloy*. Metall. Mater. Trans. A 50 (2019), pp. 3048–3060.

[20] J.W. Christian, *The Theory of Transformations in Metals and Alloys; an Advanced Textbook in Physical Metallurgy*, Pergamon Press, Oxford, 1965.

[21] P. Merle and F. Fouquet, *Coarsening of θ' plates in Al-Cu alloys—I. experimental determination of mechanisms*. Acta Metall. 29 (1981), pp. 1919–1927.

[22] E. Povoden-Karadeniz, Mobility Diffusion Data from MatCalc Database 'mc_al.ddb' version 2.006 (2015).

[23] E. Povoden-Karadeniz, Thermodynamic Data from MatCalc Database 'mc_al.tdb', version 2.030 (2015).

[24] S. Liu, E. Martínez and J. Llorca, *Prediction of the Al-rich part of the Al-Cu phase diagram using cluster expansion and statistical mechanics*. Acta Mater. 195 (2020), pp. 317–326.

[25] A. Rodríguez-Veiga, B. Bellón, I. Papadimitriou, G. Esteban-Manzanares, I. Sabirov and J. Llorca, *A multidisciplinary approach to study precipitation kinetics and hardening in an Al-4Cu (wt. %) alloy*. J. Alloys Compd. 757 (2018), pp. 504–519.